

Phase inhomogeneities in the charge-orbital-ordered manganite $\text{Nd}_{0.5}\text{Sr}_{0.5}\text{MnO}_3$ revealed through polaron dynamics

R. P. Prasankumar,^{1,*} S. Zvyagin,² K. V. Kamenev,³ G. Balakrishnan,⁴ D. Mck. Paul,⁴ A. J. Taylor,¹ and R. D. Averitt^{1,†}

¹Center for Integrated Nanotechnologies, Los Alamos National Laboratory, Los Alamos, New Mexico 87545, USA

²Dresden High Magnetic Field Laboratory (HLD), Forschungszentrum Dresden, Rossendorf, 01314 Dresden, Germany

³Center for Science at Extreme Conditions and School of Engineering and Electronics, University of Edinburgh, Mayfield Road, Edinburgh EH9 3JZ, United Kingdom

⁴Department of Physics, University of Warwick, Coventry CV4 7AL, United Kingdom

(Received 1 June 2007; published 6 July 2007)

Ultrafast midinfrared spectroscopy is used to probe dynamics in the intermediate bandwidth manganite $\text{Nd}_{0.5}\text{Sr}_{0.5}\text{MnO}_3$. In the majority paramagnetic and ferromagnetic phases, the early time dynamics are consistent with the excitation and subsequent redressing of uncorrelated lattice polarons, with longer time dynamics related to spin-lattice thermalization. These polaron excitations reveal the intrinsically inhomogeneous nature of these phases. At lower temperatures we observe ultrafast melting of charge-orbital order, liberating quasiparticles that subsequently relax into bound polaronic states on a subpicosecond time scale. The temperature-dependent amplitude of the polaron excitations scales with the volume fraction of the CE phase. Thus, polaron dynamics, as measured using ultrafast spectroscopy, serve as a sensitive probe of phase inhomogeneity.

DOI: [10.1103/PhysRevB.76.020402](https://doi.org/10.1103/PhysRevB.76.020402)

PACS number(s): 75.47.Gk, 78.47.+p

The discovery of colossal magnetoresistance (CMR) in the ferromagnetic perovskite manganites has led to a resurgence of interest in their properties, due to both the rich physics inherent to these strongly correlated systems and the potential for applications in areas such as magnetic data storage.^{1,2} More recently, attention has shifted to other areas of the phase diagram, where the manganites exhibit a variety of unusual states with a strong interplay between spin, charge, and lattice degrees of freedom.³ These include different charge-orbital ordered, antiferromagnetic, and canted insulating states, all of which can be modified by external fields.

Nanoscale phase separation has recently been shown to play an important role in the unique properties of manganites.² The existence of intrinsic phase inhomogeneities resulting from phase competition (e.g., between ferromagnetic and charge-ordered/antiferromagnetic phases) has been discovered in a variety of manganite systems by techniques including optical spectroscopy, x-ray diffraction, and neutron scattering.^{2,4-9} One example is the use of x-ray and neutron scattering experiments to detect the presence of correlated and uncorrelated Jahn-Teller (JT) polarons in the paramagnetic (PM) and ferromagnetic (FM) phases of several manganite samples.^{6,10,11} Isolated JT polarons are formed when the crystal lattice distorts around a quasiparticle to minimize the energy, localizing it in real space. As the temperature is reduced towards T_C , correlations between polarons develop, resulting in nanoscale charge-orbital ordered (COO) clusters. Polaronic effects strongly influence the magnetic, transport, and optical properties of manganites; in particular, correlated polarons are thought to be a major contributor to the CMR effect.⁶ Understanding the contribution of these nanoscale inhomogeneities to manganite physics is essential for a deeper understanding of CMR and in developing the capability to design these materials for a given application through tuning properties such as the chemical composition, temperature, and magnetic field.^{2,12}

Recently, attention has shifted from the study of static

properties to the investigation of time-dependent quasiparticle dynamics in correlated electron materials, as researchers have realized the potential of ultrafast optical measurements in understanding the underlying mechanisms governing a particular system. In particular, ultrafast spectroscopy has been used to unravel the relative contributions of charge, spin, and lattice degrees of freedom to various phenomena in transition metal oxides.¹³⁻²⁴ In this work, we use ultrafast optical-pump midinfrared (IR)-probe spectroscopy to probe quasiparticle dynamics in the perovskite manganite $\text{Nd}_{0.5}\text{Sr}_{0.5}\text{MnO}_3$ (NSMO). Our results reveal that the subpicosecond dynamics following optical excitation in NSMO are due to the excitation and recombination of uncorrelated Jahn-Teller lattice polarons. These polaron excitations reveal the presence of phase inhomogeneities in the majority PM and FM phases below T_C . Below the charge-orbital ordering temperature T_{CO} , the amplitude of the polaronic excitation scales with the volume fraction of the CE phase as determined from neutron scattering. Thus, polaron dynamics, as measured using ultrafast spectroscopy, serve as a sensitive probe of phase inhomogeneity in transition metal oxides. Furthermore, unlike other experimental techniques, ultrafast spectroscopy allows us to not only detect the presence of these inhomogeneities, but also directly measure their dynamical evolution in the time domain. These experiments augment the growing body of evidence that suggests ultrafast spectroscopy can play an important role in elucidating the physics of correlated electron materials.

The low temperature ground state of the intermediate bandwidth manganite $\text{Nd}_{0.5}\text{Sr}_{0.5}\text{MnO}_3$ exhibits real space charge ordering by alternating Mn^{3+} and Mn^{4+} ions between lattice sites. This is accompanied by orbital and checkerboard-type (CE) antiferromagnetic spin ordering below $T_{CO}=160$ K,²⁵ and A-type spin ordering below ~ 200 K.^{7,26} Upon heating above T_{CO} , NSMO undergoes a first-order phase transition to a ferromagnetic metallic state, with a concomitant structural change due to the breakdown of the charge-orbital ordered state. Finally, upon further heat-

ing above $T_C=250$ K, the sample undergoes another phase transition to the high temperature paramagnetic insulating state.

In NSMO, signatures of both uncorrelated and correlated polarons (in the form of nanoscale structural correlations) have been found in the PM and FM phases using x-ray and neutron scattering.^{4,5} Neutron diffraction and Raman scattering have also been used to show that the FM phase persists below T_{CO} along with the appearance of the A-type and CE-type AFM phases.^{7,27} The fraction of mixed phases has been shown to depend on the particular sample studied;⁷ in our sample, A-type ordering has been detected below ~ 210 K, along with CE-type ordering below ~ 160 K.²⁶ Consequently, we expected temperature-dependent time-resolved optical measurements to reveal signatures of phase inhomogeneities in NSMO.

The single crystal NSMO sample investigated in this work was prepared as described in Ref. 28, with the sample cut along the (111) axis. To optimize the surface quality, we followed a procedure similar to that described in Ref. 29, in which the sample was polished for optical measurements and subsequently annealed in an oxygen atmosphere at 1000 °C for 12 h, after which it was slowly cooled to room temperature over 66 h. Optical pump, mid-IR probe measurements were performed in reflection at near normal incidence with the pump and probe p polarized and a pump fluence of 2.16 mJ/cm² at 800 nm (1.55 eV), exciting an initial carrier density of 1.1×10^{21} cm⁻³ (~ 0.25 /unit cell); further details of the experimental setup are described elsewhere.^{22,23} The probe fluence was $<1\%$ of the pump fluence in all experiments. We utilized mid-IR probe wavelengths since the sensitivity of ultrafast spectroscopy to photo-induced phase transitions should be maximum near the optical gap, where the largest temperature-dependent changes in the reflectivity occur.³⁰ Temperature-dependent measurements were taken while cooling from room temperature to 10 K at probe wavelengths of 2.1 and 13 μ m; we will focus on the 13 μ m dynamics since the measured response was similar at both probe wavelengths.

Figure 1 depicts the photoinduced normalized change in reflectivity, $\Delta R/R$, as a function of temperature at 13 μ m (0.095 eV). At all temperatures, we observe both an ultrafast (<1 ps) component and a slow component that recovers on a longer time scale. The slow recovery matches previously published measurements^{13–18} at all temperatures and will therefore only be briefly discussed here. In the PM phase, the photoinduced reflectivity change observed at long time delays is due to the elevated sample temperature after electron-lattice thermalization.^{14,16} Upon lowering the temperature into the FM phase, the observed slow component is related to spin-lattice relaxation; this has been extensively studied in previous work on half-metallic manganite thin films.^{14–16,18} Finally, below T_{CO} the measured dynamics at long time delays are due to the melting of long range charge and orbital order, after which the COO state recovers on a nanosecond time scale through heat diffusion into the surrounding, non-photoexcited volume.^{13,17} In particular, the slow rise in $\Delta R/R$ from 10–200 ps at 110 and 50 K is due to heat diffusion from the photoexcited pump volume into the larger probe volume;³¹ this was verified by calculating the time

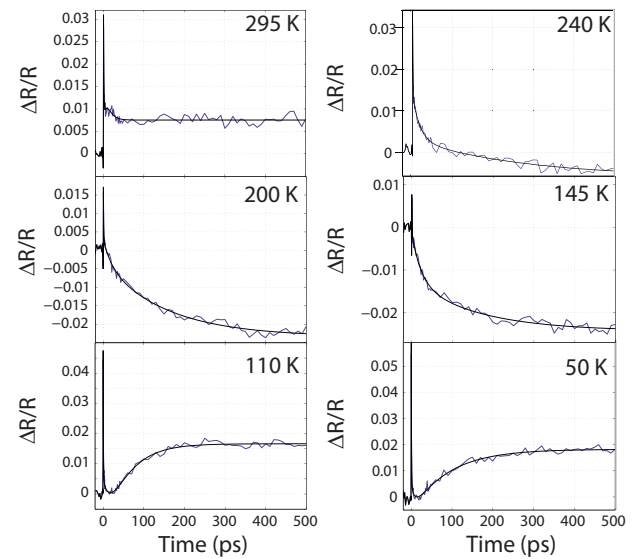


FIG. 1. (Color online) Temperature-dependent measurements on NSMO with a 13 μ m probe.

required for heat deposited within the pumped volume to diffuse into the probed volume, utilizing estimates of the sound velocity in NSMO.²⁸

The agreement of our data at long times with previously published work demonstrates that our experiments at mid-IR probe energies are sensitive to quasiparticle dynamics in NSMO. In the following, we focus on the subpicosecond dynamics in NSMO. We argue that the measured dynamics are related to a polaronic response that is, in turn, sensitive to the presence and temporal evolution of phase inhomogeneities.

Figure 2 depicts the photoinduced change in reflectivity at early times in NSMO. At high temperatures ($T > T_{CO}$), these dynamics originate from the photoexcitation and subsequent redressing of uncorrelated lattice polarons. Microscopically, this can be understood by examining time-integrated optical measurements on NSMO, in which an optical conductivity peak near 0.5 eV believed due to Jahn-Teller polaron absorp-

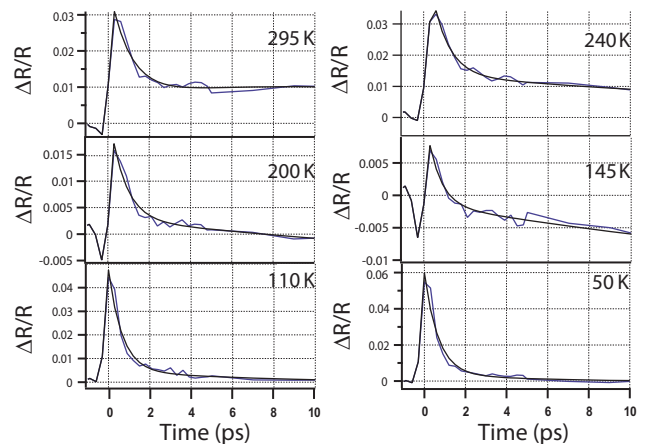


FIG. 2. (Color online) Temperature-dependent measurements on NSMO with a 13 μ m probe at early times.

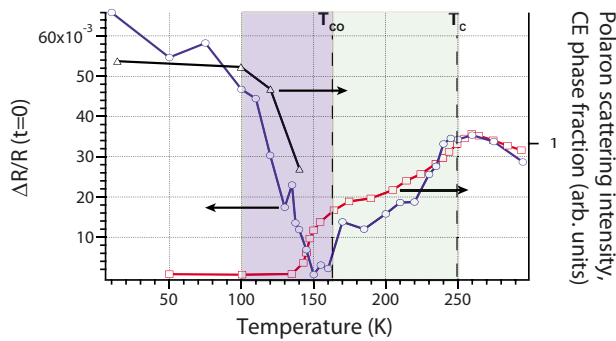


FIG. 3. (Color online) Amplitude of $\Delta R/R$ measured at $13 \mu\text{m}$ at $t=0$ ps (circles) compared to single-polaron diffuse scattering measured by x-ray diffraction (squares) [reprinted from Ref. 4 and scaled for comparison with $\Delta R/R(t=0)$] and the CE volume phase fraction (triangles) measured by neutron scattering (reprinted from Ref. 7 and scaled for comparison). The shaded areas indicate temperature ranges in which minority phases compete with the FM [green (light gray)] and COO [blue (dark gray)] dominant phases.

tion and another peak near 1.5 eV believed due to a Mn $e_g - e_g$ transition were found.^{8,30,32} In this scenario, the 1.5 eV pump pulse excites an electron from a lower e_g level to an upper e_g level, after which it will either rapidly relax on the same Mn site or hop to one or more Mn sites before relaxing.³³ The subpicosecond decay shown in Fig. 2 can be therefore attributed to the hopping and redressing of Jahn-Teller polarons.

Further support for this argument comes from comparing the temperature dependence of $\Delta R/R(t=0)$ to the number of uncorrelated lattice polarons (proportional to the single polaron scattering intensity) in the PM and FM phases as measured by x-ray scattering (Fig. 3).⁴ As described in Ref. 4, the polaron scattering intensity increases as $T \rightarrow T_C$ from above in the PM phase and continuously decreases below T_C , clearly indicating the presence of single JT polarons in the FM phase (below T_{CO} the uncorrelated polarons disappear due to the formation of long range charge-orbital order). From our data, $\Delta R/R(t=0)$ also increases as $T \rightarrow T_C$ in the PM phase. As T is lowered below T_C , the increased quasiparticle kinetic energy allows electrons to overcome polaronic trapping and freely move through the lattice, causing the photoinduced reflectivity at $t=0$ to decrease. The close correspondence between $\Delta R/R(t=0)$ and the polaron scattering intensity for $T > T_C$ strongly suggests that the initial photoinduced reflectivity increase is due to excitation of quasiparticles out of uncorrelated lattice polaronic states. The existence of these polaron excitations above T_{CO} is a direct indication of the inhomogeneous nature of the majority PM and FM phases, in contrast with measurements on optimally doped manganites in which polaron excitations vanish below T_C .^{16,33}

The ensuing sub-ps decrease in reflectivity corresponds to the time required for a photoexcited electron to redress to a polaronic state,³³ predicted by neutron and x-ray scattering measurements to be a few hundred femtoseconds.⁶ Curve fits to our data reveal the polaron redressing time to be ~ 300 fs, in good agreement with these predictions. The measured fast

relaxation time is approximately constant through the PM \rightarrow FM phase transition. This can be understood by noting that, as discussed above, the probe photon energies are sensitive to the dynamics of uncorrelated polarons, which are unaffected by the onset of spin correlations in the FM phase. Therefore, as observed in our experiments, the polaron redressing time will not change significantly across the metal-insulator transition. These measurements thus present a coherent picture of single polaron dynamics in NSMO in the paramagnetic and ferromagnetic phases, revealing the persistence of nanoscale phase inhomogeneities into the ferromagnetic regime.

We now focus on the ultrafast dynamics in the majority COO phase ($T < T_{CO}$). Neutron scattering experiments have shown that the CE phase coexists with FM and A-type AFM phases below T_{CO} , growing with decreasing temperature from a CE phase fraction of $\sim 30\%$ at 140 K until saturating at $\sim 60\%$ around 100 K (Fig. 3).⁷ In our experiments, the pump excitation instantaneously melts the CE phase, triggering an insulator-to-metal transition (IMT) similar to that induced by a magnetic field.^{13,17,25} This photoinduced phase transition closes the optical conductivity gap on an ultrafast time scale and causes the initial increase in $\Delta R/R(t=0)$. This interpretation is supported by examining the temperature dependence of $\Delta R/R(t=0)$ (Fig. 3), which is nearly zero at T_{CO} but increases with decreasing T in the COO state, finally saturating below 100 K. Figure 3 shows that the CE phase fraction follows the same temperature dependence, implying that the $\Delta R/R(t=0)$ signal is a direct measure of the CE phase fraction at a given temperature below T_{CO} .

The subpicosecond recovery in the COO state following photoexcitation also corresponds to the redressing of uncorrelated JT polarons. Previous investigations of ultrafast dynamics in charge-orbital-ordered manganites have demonstrated that the COO state recovers on a time scale of several nanoseconds after optical excitation.^{13,17} Therefore, the sub-ps relaxation shown in Fig. 2 for $T < T_{CO}$ does not correspond to the recovery of charge and orbital order, but rather is due to relaxation of the nonequilibrium quasiparticles into uncorrelated JT polaronic states. Indeed, the dynamics after the pump excitation are similar to that observed in the PM and FM phases; as at high temperatures, electrons initially excited on Mn³⁺ sites can rapidly hop to other sites, which disorders the COO state within the pump penetration depth of ~ 60 nm. The photoexcited electrons are then trapped by lattice distortions, redressing them into polaronic states and transferring their energy to the lattice within 4 ps (when $\Delta R/R$ returns to zero). As previously described, heat then propagates from the photoexcited pump volume into the much larger probe volume, causing $\Delta R/R$ to rise at longer time delays.³¹

We find that as T is progressively lowered, the polaron redressing time increases around T_{CO} and continues to do so until ~ 100 K (saturating at ~ 700 fs). This may be due to the phase transition induced by the pump pulse when $T < T_{CO}$; the structural change associated with the photoinduced phase transition changes the electron-phonon coupling strength and therefore the polaron redressing time. Finally, it is worth noting that our experiments are not sensitive to the dynamics of correlated polarons at any temperature since the optical ex-

citation would melt COO clusters, liberating quasiparticles that would quickly relax into uncorrelated polaronic states as described above.

In conclusion, we have utilized ultrafast midinfrared spectroscopy to probe quasiparticle dynamics in the COO manganite $\text{Nd}_{0.5}\text{Sr}_{0.5}\text{MnO}_3$. We find that the dynamics on long time scales are consistent with previously published results, demonstrating our ability to sensitively probe manganite physics at mid-IR wavelengths. Ultrafast mid-IR spectroscopy allows us to track the evolution of uncorrelated Jahn-Teller polarons in the PM and FM phases from their excitation out of bound states to their subsequent redressing within ~ 300 fs. The existence of these polaronic excitations above T_{CO} reveals the intrinsically inhomogeneous nature of the PM and FM phases. Below T_{CO} , the pump pulse melts the charge-orbital ordered state, initiating an ultrafast insulator-to-metal transition. The subsequent dynamics are nearly

identical to that observed at high temperatures, as we again observe the redressing of photoexcited quasiparticles into uncorrelated polaronic states. Finally, we find that the amplitude of this polaronic excitation is a direct measure of the CE phase fraction below T_{CO} . These experiments strongly suggest that ultrafast spectroscopy is sensitive to the presence of phase inhomogeneities in transition metal oxides, and in contrast with other techniques, can directly measure their dynamics in the time domain. Future experiments, such as time-resolved near-field optical microscopy, should provide further insight into the nature of nanoscale phase separation in strongly correlated systems.

We would like to acknowledge H. J. Lee for experimental assistance, B. S. Kang for help with sample annealing, and J. H. Jung for providing time-integrated reflectivity data.

*rpprasan@lanl.gov

[†]Present address: Department of Physics, Boston University, 590 Commonwealth Avenue, Boston, Massachusetts 02215, USA.

¹*Colossal Magnetoresistive Oxides*, edited by Y. Tokura (Gordon and Breach, Amsterdam, 2000).

²E. Dagotto, *Nanoscale Phase Separation and Colossal Magnetoresistance* (Springer, Berlin, 2003).

³C. N. R. Rao, A. Arulraj, A. K. Cheethan, and B. Raveau, *J. Phys.: Condens. Matter* **12**, R83 (2000).

⁴V. Kiryukhin, B. G. Kim, T. Katsufuji, J. P. Hill, and S.-W. Cheong, *Phys. Rev. B* **63**, 144406 (2001).

⁵V. Kiryukhin, T. Y. Koo, A. Borissov, Y. J. Kim, C. S. Nelson, J. P. Hill, D. Gibbs, and S.-W. Cheong, *Phys. Rev. B* **65**, 094421 (2002).

⁶V. Kiryukhin, *New J. Phys.* **6**, 155 (2005).

⁷P. M. Woodward, D. E. Cox, T. Vogt, C. N. R. Rao, and A. K. Cheetham, *Chem. Mater.* **11**, 3528 (1999).

⁸J. H. Jung, H. J. Lee, T. W. Noh, E. J. Choi, Y. Moritomo, Y. J. Wang, and X. Wei, *Phys. Rev. B* **62**, 481 (2000).

⁹H. J. Lee, K. H. Kim, M. W. Kim, T. W. Noh, B. G. Kim, T. Y. Koo, S.-W. Cheong, Y. J. Wang, and X. Wei, *Phys. Rev. B* **65**, 115118 (2002).

¹⁰S. Shimomura, N. Wakabayashi, H. Kuwahara, and Y. Tokura, *Phys. Rev. Lett.* **83**, 4389 (1999).

¹¹C. P. Adams, J. W. Lynn, Y. M. Mukovskii, A. Arsenov, and D. A. Shulyatev, *Phys. Rev. Lett.* **85**, 3954 (2000).

¹²A. Millis, *Nature (London)* **392**, 147 (1998).

¹³M. Fiebig, K. Miyano, Y. Tomioka, and Y. Tokura, *Appl. Phys. B: Lasers Opt.* **B71**, 211 (2000).

¹⁴A. I. Lobad, R. D. Averitt, C. Kwon, and A. J. Taylor, *Appl. Phys. Lett.* **77**, 4025 (2000).

¹⁵R. D. Averitt, A. I. Lobad, C. Kwon, S. A. Trugman, V. K. Thorsmolle, and A. J. Taylor, *Phys. Rev. Lett.* **87**, 017401 (2001).

¹⁶R. D. Averitt and A. J. Taylor, *J. Phys.: Condens. Matter* **14**, R1357 (2002).

¹⁷T. Ogasawara, K. Tobe, T. Kimura, H. Okamoto, and Y. Tokura, *J. Phys. Soc. Jpn.* **71**, 2380 (2002).

¹⁸T. Ogasawara, M. Matsubara, Y. Tomioka, M. Kuwata-Gonokami, H. Okamoto, and Y. Tokura, *Phys. Rev. B* **68**, 180407(R) (2003).

¹⁹S. Tomimoto, S. Miyasaka, T. Ogasawara, H. Okamoto, and Y. Tokura, *Phys. Rev. B* **68**, 035106 (2003).

²⁰T. Mertelj, D. Mihailovic, Z. Jaglicic, A. A. Bosak, O. Yu. Gorbunenko, and A. R. Kaul, *Phys. Rev. B* **68**, 125112 (2003).

²¹S. A. McGill, R. I. Miller, O. N. Torrens, A. Mamchik, I.-Wei Chen, and J. M. Kikkawa, *Phys. Rev. Lett.* **93**, 047402 (2004).

²²R. P. Prasankumar, H. Okamura, H. Imai, Y. Shimakawa, Y. Kubo, S. A. Trugman, A. J. Taylor, and R. D. Averitt, *Phys. Rev. Lett.* **95**, 267404 (2005).

²³D. J. Hilton, R. P. Prasankumar, S. A. Trugman, A. J. Taylor, and R. D. Averitt, *J. Phys. Soc. Jpn.* **75**, 011006 (2006).

²⁴K. Miyasaka, M. Nakamura, Y. Ogimoto, H. Tamaru, and K. Miyano, *Phys. Rev. B* **74**, 012401 (2006).

²⁵H. Kuwahara, Y. Tomioka, A. Asamitsu, Y. Moritomo, and Y. Tokura, *Science* **270**, 961 (1995).

²⁶S. Zvyagin, A. Angerhofer, K. V. Kamenev, L.-C. Brunel, G. Balakrishnan, and D. Mck. Paul, *Solid State Commun.* **121**, 117 (2002).

²⁷K.-Y. Choi, P. Lemmens, G. Guntherodt, M. Pattabiraman, G. Rangarajan, V. P. Gnezdilov, G. Balakrishnan, D. McK. Paul, and M. R. Lees, *J. Phys.: Condens. Matter* **15**, 3333 (2003).

²⁸S. Zvyagin, H. Schwenk, B. Luthi, K. V. Kamenev, G. Balakrishnan, D. McK. Paul, V. I. Kamenev, and Y. G. Pashkevich, *Phys. Rev. B* **62**, R6104 (2000).

²⁹K. Tobe, T. Kimura, and Y. Tokura, *Phys. Rev. B* **69**, 014407(1) (2004).

³⁰J. H. Jung (private communication).

³¹In optical-pump mid-IR probe experiments, it is important to account for the difference in penetration depths between the pump and probe wavelengths. For example, in NSMO the 800 nm pump has a penetration depth of ~ 60 nm while the penetration depth of the $13 \mu\text{m}$ probe is $1.33 \mu\text{m}$ at 15 K. This can result in transients due to heat diffusion between the pumped and probed volumes.

³²M. Quijada, J. Cerne, J. R. Simpson, H. D. Drew, K. H. Ahn, A. J. Millis, R. Shreekala, R. Ramesh, M. Rajeswari, and T. Venkatesan, *Phys. Rev. B* **58**, 16093 (1998).

³³H. J. Lee, R. D. Averitt, S. A. Trugman, J. Demsar, D. J. Funk, N. H. Hur, Y. Moritomo, and A. J. Taylor (unpublished).